Accepted Manuscript

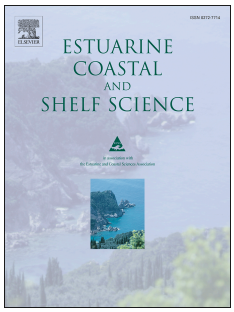

A winter dinoflagellate bloom drives high rates of primary production in a Patagonian fjord ecosystem

P. Montero, I. Pérez-Santos, G. Daneri, M.H. Gutiérrez, G. Igor, R. Seguel, D. Purdie, D.W. Crawford

PII: S0272-7714(16)30805-8

DOI: 10.1016/j.ecss.2017.09.027

Reference: YECSS 5629

To appear in: *Estuarine, Coastal and Shelf Science*

Received Date: 31 December 2016

Revised Date: 7 September 2017

Accepted Date: 26 September 2017

Please cite this article as: Montero, P., Pérez-Santos, I., Daneri, G., Gutiérrez, M.H., Igor, G., Seguel, R., Purdie, D., Crawford, D.W., A winter dinoflagellate bloom drives high rates of primary production in a Patagonian fjord ecosystem, *Estuarine, Coastal and Shelf Science* (2017), doi: 10.1016/j.ecss.2017.09.027.

A winter dinoflagellate bloom drives high rates of primary production in a Patagonian fjord ecosystem

P. Montero[1,2], I. Pérez-Santos[3,2*], G. Daneri[1,2], M. H. Gutiérrez[2,4], G. Igor[1,2], R. Seguel[3], D. Purdie[5], D. W. Crawford[1]

[1]Centro de Investigación en Ecosistemas de la Patagonia (CIEP), Coyhaique, Chile

[2]COPAS Sur–Austral, Universidad de Concepción, Concepción, Chile

[3]Centro i~mar, Universidad de Los Lagos, Puerto Montt, Chile

[4]Departamento de Oceanografía, Universidad de Concepción, Concepción, Chile

[5]Ocean and Earth Science, National Oceanography Centre Southampton, University of Southampton, United Kingdom.

*Corresponding author:

E-mail address: ivan.perez@ulagos.cl (I. Pérez-Santos)

Abstract

A dense winter bloom of the dinoflagellate *Heterocapsa triquetra* was observed at a fixed station (44°35.3'S; 72°43.6'W) in the Puyuhuapi Fjord in Chilean Patagonia during July 2015. *H. triquetra* dominated the phytoplankton community in the surface waters between 2 and 15 m (13-58 $\times$ 10^9 cell m^{-2}), with abundances some 3 to 15 times higher than the total abundance of the diatom assemblage, which was dominated by *Skeletonema* spp. The high abundance of dinoflagellates was reflected in high rates of gross primary production (GPP; 0.6-1.6 g C m^{-2} d^{-1}) and chlorophyll-a concentration (Chl-a; 70-199.2 mg m^{-2}) that are comparable to levels reported in spring diatom blooms in similar Patagonian fjords. We identify the main forcing factors behind a pulse of organic matter production during the non-productive winter season, and test the hypothesis that low irradiance levels are a key factor limiting phytoplankton blooms and subsequent productivity during winter.

Principal Component Analysis (PCA) indicated that GPP rates were significantly correlated ($r = -0.8$, $p < 0.05$) with a decrease in salinity/temperature and the presence of the *Heterocapsa* bloom. The bloom occurred under low surface irradiance levels characteristic of austral winter and was accompanied by strong northern winds, associated with the passage of a low-pressure system, and a water column dominated by double diffusive layering. To our knowledge, this is the first report of a dense dinoflagellate bloom during deep austral winter in a Patagonian fjord, and our data challenge the paradigm of light limitation as a factor controlling phytoplankton blooms in this region in winter.

Keywords: primary production, mixing, winter dinoflagellate blooms, Patagonian fjord

1. Introduction

In coastal waters around the world, dinoflagellate blooms have been typically associated with stratification of the water column during summer (Margalef, 1978; Legendre, 1990; Casas et al., 1999; Barton et al., 2013). However, in some estuaries of the northern hemisphere high abundances of these organisms have also been reported in winter, and can at times contribute significantly to annual phytoplankton carbon production (Sellner et al., 1991; Litaker et al., 2002 a, b; Marshall et al. 2005). The dinoflagellates involved have clearly been able to thrive under some of the conditions encountered in winter such as relatively low temperature and irradiance (Litaker et al., 2002 a, b), high nutrient availability, low grazing pressure and a stratified water column (Cohen, 1985, Litaker et al., 2002 a, b; Millette et al., 2015).

The thecate dinoflagellate *Heterocapsa triquetra* is one of the most common winter bloom-forming species found in estuarine ecosystems (Baek et al. 2011), with low temperatures and strong atmospheric frontal systems in winter somehow creating a favorable niche for this species (Litaker et al. 2002 a, b). Some species of *Heterocapsa* in cultures are able to grow at temperatures below 10 ºC, and even below 0º C (Yamaguchi et al., 1997; Baek et al., 2011; Tas, 2015), and so may benefit from the seasonal drop in water temperature that might potentially reduce the presence of mesozooplankton grazers (Millette et al., 2015). In the northern hemisphere, low-pressure systems are accompanied by regular rainfall and terrestrial runoff that supplies inorganic nutrients critical for initiation and development of these blooms (Litaker et al., 2002a). According to Mallin et al. (1991), Mallin (1994) and Baek et al. (2011), low salinity and high nitrate concentrations, resulting from heavy rains during winter, appear to be crucial for formation of blooms of *Heterocapsa triquetra*. Indeed, *H. triquetra* has a high rate of uptake and assimilation of nitrate (Mallin et al., 1991; Mallin 1994), is

tolerant of a wide range of salinities (10-40) (Lee at al., 2005), and might therefore be specifically favored by the environmental conditions encountered in winter.

In Patagonian fjords, winter conditions differ from the estuaries of the northern hemisphere, because increased freshwater input generally results in surface waters having high concentrations of silicic acid (Silva, 2008; Torres et al., 2014) but low concentrations of nitrate and phosphate (Silva, 2008; Silva and Vargas, 2014). Fertilization of surface fjord waters therefore requires increased supply of nitrate and phosphate from deeper waters through vertical mixing of the water column (Goebel et al., 2005), and this process may be strongly modulated by the passage of low-pressure systems during winter.

The general pattern of phytoplankton succession in the fjords of southern Chile is one of dominance by small flagellates (size range: 2–20 µm) during winter (Czypionka et al., 2011), a conspicuous diatom bloom in spring, followed by increased abundances of dinoflagellates in summer and early fall (Iriarte et al., 2005; Iriarte and Gonzalez, 2008). This phytoplankton succession is consistent with the "Mandala" adopted by Margalef (1978) to conceptualize the role of nutrients and turbulence in phytoplankton growth strategies, where dinoflagellate blooms tend to develop in late summer under relatively nutrient-poor and low turbulence conditions. Blooms of *Heterocapsa triquetra* are not common in Patagonian fjords, and to date have been reported only during austral summer (Cassis et al., 2002). No other dinoflagellate has been previously reported to bloom during the deep Patagonian winter. Whereas spring blooms of diatoms such as *Skeletenoma*, are related to high levels of primary production (Iriarte et al., 2007b; Montero et al., 2011) and downward transfer of particulate organic carbon in Patagonian fjords (Iriarte et al., 2007b; González et al., 2010; Montero et al., 2011; Iriarte et al. 2013), dinoflagellate blooms appear to contribute poorly to export of

organic matter and are more associated with recycling of carbon in near-surface waters (Iriarte et al., 2005; Iriarte et al., 2007a).

In Patagonian fjords and channels, irradiance is one of the principal factors regulating the annual cycle of primary productivity (Iriarte and González, 2008) which is typically divided into productive (late winter/ early spring to late fall) and non-productive (winter) periods (Montero et al., 2011), and with most interest largely focused on the spring diatom bloom. Productivity during winter in Patagonia fjords has up to now been assumed to be limited by low temperatures and unfavorable light conditions, and therefore largely ignored, with the assumption that the winter period makes an insignificant contribution to total annual primary productivity, as generally found elsewhere (Sellner et al., 1991).

The mixing-stratification cycle is an important mechanism for controlling total phytoplankton production (Legendre and Razzoulzadegan, 1996) principally by regulating the light climate experienced by cells in the upper water column, as well as the supply of nutrients from deeper waters. In Patagonian fjords, water column mixing and destabilization can be driven by winds and the passage of low pressure systems, and therefore winter conditions could represent a favorable scenario for injection of nitrate and phosphate into surface waters, potentially stimulating phytoplankton production, as long as the irradiance levels are favorable.

A multidisciplinary sampling campaign was conducted in Puyuhuapi Fjord during July 2015 aiming to (1) identify the main forcing factors behind a pulse of organic matter production during the non-productive winter season, and (2) test the hypothesis that low irradiance levels are a key factor limiting phytoplankton blooms and subsequent productivity during winter.

2. Data and Methodology

2.1. Study area

The study was conducted in the northern section of Puyuhuapi Fjord (Fig. 1A) at a fixed station where an oceanographic and meteorological buoy (44°35.3' S; 72°43.6' W) has been operational since 2012. The buoy has been moored at ~200-meter depth and ca. 20 km NW of the mouth of the Cisnes River (Fig. 1B). Puyuhuapi Fjord runs in a N-NE direction and connects directly to the open sea via the Moraleda channel at its mouth, and through the Jacaf channel near the head (Schneider et al., 2014). The hydrography of the fjord is characterized by an estuarine type of circulation with a vertical two layer structure comprised of a highly variable 5-10 m deep freshwater layer overlying a more uniform, saltier sub-pycnocline layer (Schneider et al., 2014 and references therein). The deeper saline water originates from Sub-Antarctic Surface Water (SAAW) characteristic of open ocean environments in these latitudes (Chaigneau and Pizarro, 2005). The freshwater upper layer is mainly supplied by the Cisnes River and rain runoff (Schneider et al., 2014). The surface outflow of buoyant freshwater carries high concentrations of silicic acid derived from rivers, while SAAW waters are typically enriched with nitrate and orthophosphate (Silva 2008). Surface salinity distribution in Puyuhuapi Fjord; with higher salinity in the north than in the south, suggests an intrusion of oceanic surface waters from the north via Jacaf Channel forced by westerly winds (Schneider et al., 2014).

We conducted a winter sampling campaign from 10 to 16 July 2015 at the Puyuhuapi Fjord station, where hydrographic profiles and water samples from different depths were collected every two days. In addition, between July 5 and July 17, 2015 data was continuously recorded by the buoy at the Puyuhuapi Fjord and at the nearby meteorological station.

2.2. Atmospheric and sea-surface data

The atmospheric data was recorded every 15 minutes with a meteorological station model HOBO U-30 (44° 35.46' S / 72° 44.21' W), located on land approximately 900 m distance from the buoy. In the water column, temperature, salinity, pH, dissolved oxygen and chlorophyll-a were recorded once per hour using a YSI model 6600 V2-4 multiparameter probe deployed at ~1 m depth below the buoy. Data were averaged for each day to eliminate the influence of semidiurnal tides and other high frequency forcings in the study area (Schneider *et al*., 2014). The discharge of the Cisnes River, with an hourly temporal resolution, was obtained from the Chilean Direction of Water (www.dga.cl).

2.3. Hydrography and micro-profiler measurements

Vertical profiles of temperature, salinity and fluorescence (WET Labs sensor) were recorded using a CTD SeaBird 25 at 8 Hz. Additionally, micro-profiler measurements were carried out with a Self Contained Autonomous Micro Profiler (SCAMP) in order to evaluate mixing processes and examine micro-layers of fluorescence. The SCAMP profiler recorded data at 100 Hz, or about 1 mm vertical resolution with a descending free fall speed of ~10 cm s^{-1} and is equipped with a fast conductivity (accuracy of ±5% of the full conductivity scale) and a fast temperature response sensor (accuracy of 0.010° C). The vertical gradients of temperature measurements were used to calculate dissipation rate of turbulent kinetic energy (ε) applying the Batchelor spectrum (Ruddick et al., 2000; Luketina and Imberger, 2001).

Using the dissipation rate of turbulent kinetic energy from the SCAMP profiler, the diapycnal eddy diffusivity (K_ρ) was calculated. The most commonly used formulation for estimation of K_ρ, was proposed by Osborn (1980):

$$K_\rho = \Gamma \frac{\varepsilon}{N^2}, \quad (1)$$

where Γ is the mixing efficiency, generally set to 0.2 (Thorpe 2005), and N is the buoyancy frequency. Shih et al. (2005) noted that when the ratio $\varepsilon / \nu N^2$, with viscosity $\nu = 1.9 \times 10^{-6}$ m^2 s^{-1}, is larger than 100, the Osborn equation results in an overestimation. They propose a new parameterization for this case given by:

$$K_\rho = 2\nu \left(\frac{\varepsilon}{\nu N^2}\right)^{1/2}. \quad (2)$$

In this investigation we therefore applied equation (2) when $\varepsilon / \nu N^2 > 100$, equation (1) when $7 < \varepsilon / \nu N^2 < 100$, and considered null eddy diffusivity when $\varepsilon / \nu N^2 < 7$ (Cuypers et al., 2011).

The hydrographic data (profiles of temperature and salinity) was used to calculated the Turner angle (*Tu*, expressed in degrees of rotation) in order to determine the contributions of the double-diffusive layering (DL) process to the vertical mixing of the water column, and also to quantify the influence of temperature and salinity in the stratification of the water column (Ruddick, 1983). You (2002) proposed: when *Tu* is between -45° and -90° then DL is possible. When *Tu* is between -45° and 45° the water column is stable with respect to both temperature and salinity; and when *Tu* is between 45° and 90, salt fingering structures can be expected. According to this classification, DL can also be divided into strong (*Tu* between -90° and -75°), medium (*Tu* between -75° and -60°) and weak (*Tu* between -60° and -45°). Profiles of temperature and salinity were averaged every 1 m for SCAMP measurements to compute the *Tu* parameter.

2.4. Nutrients, chlorophyll-a and phytoplankton composition

Water samples for analyses of inorganic nutrients, chlorophyll-a (Chl-*a*) and phytoplankton abundance were collected each sampling day from 3 discrete depths (2, 5 and 15 m) using a 10-liter Niskin bottle. Additional nutrient samples were collected from 50 and 100 m depths. Samples for nutrient analyses were filtered through GF/F filters and frozen at –20 °C prior to analysis in the laboratory. Concentrations of nitrate, orthophosphate, and silicic acid were determined spectrophotometrically according to methods given in Strickland and Parsons (1968).

For Chl-*a* determinations, samples were fractionated into the following three size classes of phytoplankton: microphytoplankton (>20 μm), nanophytoplankton (2–20 μm), and picophytoplankton (<2 μm). This fractionation procedure was performed in three sequential steps: (1) for the nanophytoplankton fraction (2– 20 μm), 100 mL seawater was pre-filtered using 20-μm Nitex mesh and collected on a 2.0-μm Nuclepore filter; (2) for the picoplankton fraction (0.2-2.0 μm), the filtrate from the 2.0-μm Nuclepore filter in step (1) was filtered again onto a 0.7-μm MFS (Microfiltration Systems) glass-fiber filter; (3) for the whole phytoplankton community, 100 mL seawater was filtered through a 0.7-μm MFS glass-fiber filter. The microphytoplankton fraction was obtained by subtracting the estimated Chl-a in steps (1) and (2) from the estimates in step (3). Filters were immediately frozen (–20 ºC) until later analysis; pigments were extracted with 90% v/v acetone and measured using a Turner Design TD-700 fluorometer according to standard procedures (Parsons et al., 1984). Depth-integrated values of Chl-a were calculated down to 15 m, using trapezoidal integration.

Samples for phytoplankton cell counts were stored in 250 ml clear plastic bottles, and preserved in a 1% Lugol's iodine solution (alkaline). From each sample, a 10-mL sub-sample was placed in a sedimentation chamber and allowed to settle for 12 h (Utermöhl, 1958) prior to identification at 40X and 100X using an inverted microscope

(Carl Zeiss, Axio Observer A.1). Fifty random fields were counted for each sample. Estimates of phytoplankton abundance at the three discrete depths were integrated down to 15 m, using a trapezoidal method.

2.5. Primary production

During each sampling day, *in situ* experiments were conducted to measure gross primary production (GPP). A total of 4 experiments were conducted during the study period and incubations were performed on water samples obtained from the same sampling depths indicated above (2, 5 and 15 m). GPP was estimated from changes in dissolved oxygen concentrations observed during *in situ* incubation of light and dark bottles (Strickland, 1960). Water from the Niskin bottle was transferred into 125 mL (nominal volume) borosilicate bottles (gravimetrically calibrated) using a silicone tube, whilst taking care to exclude air bubbles. Five time-zero bottles, five light bottles, and five dark bottles were used for each incubation depth. Time-zero bottles were fixed at the beginning of each experiment, whereas the light and dark bottles were incubated *in situ* attached to a surface-tethered mooring system. Water samples were collected at dawn and were incubated during the whole light period (incubating time was 7.0 ± 0.8 hours). Dissolved oxygen concentrations were determined according to the Winkler method (Strickland and Parsons, 1968), using a Metrohom burette (Dosimat plus 865) and by automatic visual end-point detection (AULOX Measurement System). Daily GPP rates were calculated as follows: GPP = (mean [O_2] light bottles – mean [O_2] dark bottles). GPP values were converted from oxygen to carbon units using a conservative photosynthetic quotient (PQ) of 1.25 (Williams and Robertson, 1991). Discrete-depth estimates of GPP rates were integrated down to 15 m, using a trapezoidal method.

2.6. Statistical analyses

A principal component analysis (PCA) was performed to combine the variables chl-a, inorganic nutrients, temperature, salinity, dissolved oxygen concentration, photosynthetically active radiation (PAR) and abundance of phytoplankton species, into statistically independent environmental predictors for GPP values. The data used in this analysis corresponded to values obtained at each sampling depth during the study period. A Spearman correlation analysis (r_s) was then conducted to assess the degree of association between these principal components and log-transformed GPP values.

3. Results

3.1. Atmospheric and sea-surface conditions

Atmospheric conditions observed during the sampling period showed evidence of the passage of multiple low-pressure systems (LPS), characterized by north winds with intensities ranging from 5 to 20 m s^{-1} and low atmospheric pressure (Fig. 2 A-B), and leaving an identifiable signal in the Cisnes River discharge (Fig. 2C). During the days of the study, surface water temperature and salinity (Fig. 2D and 2E) decreased during the passage of LPS (temperature 7-9° C and salinity 10-15), whereas surface dissolved oxygen increased from 8 mL L^{-1} to 13 mL L^{-1} (Fig. 2F), possibly in response to the high surface values of chl-a (100 to >150 µg L^{-1}), (Fig. 2G). High surface pH values (8.5-9.2) were also recorded during periods where chl-a was high (Fig. 2H).

3.2. Hydrography and vertical mixing

The hydrography of Puyuhuapi Fjord was characterized by a vertical two-layer structure with a highly variable 0–10 m freshwater surface and a more uniform saltier lower layer (Fig. 3B). Brackish or saline estuarine waters (salinity < 31; Sievers and

Silva, 2008) occupied the upper (0-20 m) layer of the water column while the deeper (20-40 m) layer showed a Modified Sub-Antarctic Water (MSAAW; Sievers and Silva, 2008), with salinities ~31 and temperatures around 11ºC. Temperature and salinity increased from surface to deeper waters during study period (Fig. 3A, B). The surface layer was colder than the deeper layer (Fig. 3A), thus resulting in a thermal inversion characteristic of winter months (Schneider et al., 2014).

A shallow pycnocline (~2 m) was observed during the days before and after (12th and 16th) the passage of the LPS on July 15, 2015, with a further step in density at 6.5 m (Fig. 3C). These density changes generated high buoyancy frequency within the pycnocline zone with values ranging from 0.01-0.02 s^{-2} (Fig. 3D). The shallower maximum of buoyancy frequency disappeared on July 15, and the slightly deeper maximum also decreased in intensity in response to the vertical homogenization of temperature and salinity (Fig. 3A, B), reflecting the water column mixing driven by the passage of the LPS. The water column was influenced by wind driven mixing down to approximately 30 m depth, but particularly above 7 m, with surface temperature and salinity increasing around 1.5° C and 5, respectively on July 15 (Fig. 3A, B). The temperature gradient was high from the surface down to 17 m depth with a variation of between -2 and 2 °C m^{-1} (Fig. 3E).

The gradient of temperature and salinity with depth favored the occurrence of double-diffusive layering (DL) in 84% of the total data points with Turner angle values between -75° and -45° (Fig. 3F). The remaining 16 % of the Turner angle data were between -45° and 45° (not shown on figure), corresponding to a stable water column with respect to temperature and salinity. In the diffusive layer, high values of dissipation rate of turbulent kinetic energy (ε) were obtained ranging from 10^{-5} to 10^{-4} W kg^{-1} (Fig. 3G). Before (black line) and after (red line) the influence of the LPS, the high values for

ε were recorded between 4 and 21 m depth with maximum of $\varepsilon=4.8 \times 10^{-4}$ W kg^{-1} and values decreased to the bottom ($\varepsilon=10^{-9}$ - 10^{-5} W kg^{-1}). Hours after the passage of the LPS (blue line), the dissipation rate of turbulent kinetic energy showed two maxima, at 5 and 15 m depth with $\varepsilon=5.1 \times 10^{-4}$ W kg^{-1}, and then ε diminished abruptly to $\varepsilon= 10^{-9}$ - 10^{-8} W kg^{-1} deeper in the water column. In response to the high ε (0-20 m), elevated values of diapycnal eddy diffusivity were obtained (3.5×10^{-3} m^2 s^{-1}) (Fig. 3H).

3.3. Nutrient measurements

Concentrations of nitrate <10 µM and low phosphate values (<0.2 µM) were observed within the top 5 m of water column. Below this layer and between 15 and 100 m depth, nitrate levels fluctuated between 9 and 21 µM and phosphate between 0.6 and 1.8 µM (Table 1). Silicic acid concentrations were higher (33-71 µM) within the top 5 m of water column than in deeper waters (19-60 µM) (Table 1), coinciding with the input of low-salinity water (Fig. 3B).

3.4. Phytoplankton community composition, chlorophyll-a and primary production

High depth-integrated total phytoplankton abundance (18-63 $\times 10^9$ cell m^{-2}) and chl-a concentration (70-199.2 mg Chl-*a* m^{-2}) were observed during the study period, with a clear dominance (13-58 $\times 10^9$ cell m^{-2}) by the dinoflagellate *Heterocapsa triquetra* and an almost complete absence of coexisting phytoplankton species (Fig. 4A). Diatoms were poorly represented in depth integrated totals in the water column, and consisted mainly of *Skeletonema* spp. (2-4 $\times 10^9$ cell m^{-2}) (Fig. 4A). Higher abundances of phytoplankton (1-9 $\times 10^3$ cell mL^{-1}) were observed in near-surface (2-5 m) than in subsurface (15 m) waters (<1 $\times 10^3$ cell mL^{-1}) (Table 1). Consistently, in-situ measurements of chl-a ranged between 5.1-28.5 µg L^{-1} in surface water (2-5 m) and

between 1.7-4.2 µg L^{-1} at 15 m depth (Table 1). Total Chl-*a* was dominated by the nanophytoplankton (2-20 µm) and microphytoplankton (>20 µm) fractions, with a very low proportion made up by the picophytoplankton (<2 µm) fraction (Fig. 4B).

GPP rates derived from O_2 incubations were higher (2.6-31.4 mmol O_2 m^{-3} d^{-1}) at 2 and 5 m than at 15 m (0.2-9.4 mmol O_2 m^{-3} d^{-1}) (Table 1), with values of depth-integrated GPP ranging from 0.6 to 1.6 g C m^{-2} d^{-1} over the study period (Fig. 4A).

Principal component analysis (PCA) showed first (PC-1) and second principal component (PC-2) explaining 64.9% and 13.9 % of total variance, respectively (Fig. 5A). PC-1 was positively loaded with salinity, temperature, phosphate and nitrate, while Chl-a, silicic acid, dissolved oxygen and abundance of *Heterocapsa triquetra* were found to be negatively loaded. The PC-2 was shown to be related to a few variables, with abundance of *Skeletonema* spp. and silicic acid positively loaded and PAR negatively loaded (Fig. 5A).

The PCA analysis clearly showed an ordination of sampling sites according to depth, which involves the distribution of light (PAR) and the vertical separation in the sources of silicic acid from surface freshwater, and nitrate and phosphate from deeper oceanic water (Fig. 5A). In this ordination, and, as shown by fluorescence profile (Fig. 6), the highest concentration of phytoplankton was in surface waters (0-8 m above pycnocline). GPP was significantly correlated with PC-1 (r_s=-0.8, n=12, p<0.05) but not with PC-2 (r_s=0.07, n=12, p>0.05) (Fig. 5B).

3.5. Vertical profiles of fluorescence

The data recorded by the fluorescence sensor on the CTD was used to describe changes in the relative position of the maximum of chl-a over the sampling period (Fig. 6). This data showed an absolute maximum of 104.3 mg m^{-3} chl-a at 1.5 m depth during

July 12 at midday, but more generally, fluorescence maxima ranged from 20 to 50 mg m^{-3} chl-a and were concentrated in the upper few metres (Fig. 6). The PAR profiles presented demonstrate the low level of irradiance registered during this winter campaign, compared with other records from late spring 2013 and summer 2014 (Fig. 6) within the same study area.

The SCAMP microprofiler obtained high vertical resolution in profiles of fluorescence (units in voltage) that allowed the detection of a peculiar behavior of the dinoflagellate *Heterocapsa triquetra*, which was dominating the bloom. (1) During sunrise at 9:29 of July 12, a double maximum of fluorescence was recorded in the upper five meters of the water column, at 1.5 m and 3 m (supplementary material, Fig. 1). Over time, the double maximum merged into one peak by 15:07. The double maximum structure was again detected at 8:00 during July 16 (supplementary material, Fig. 2) showing a similar behavior with time. (2) A deepening of the fluorescence maximum to 8 m depth was recorded in the afternoon at 16:06 on July 15, hours after the passage of the low pressure system, and coinciding with the displacement of the pycnocline by vertical mixing (supplementary material, Fig. 1). In general the fluorescence peaks were observed over the position of the pycnocline. (3) A vertical migration pattern of the fluorescence peak was distinguished in all SCAMP profiles. At sunrise, the algae were concentrated between 2-5 m depth and started to ascend from 10:00 to 12:00. By noon, the maximum florescence peak reached very close to the surface and remained within the first 2 m, above the pycnocline (supplementary material, Fig. 2). The in-situ sampling confirmed that the phytoplankton assemblage was dominated by high abundance of *Heterocapsa triquetra* (2-8 $\times$ 10^3 cell mL^{-1}) above the pycnocline (supplementary material, Fig. 1 and Fig. 2). The position of the maximum in cell abundance agreed with the fluorescence peak, particularly during the double maximum

distribution, and this was supported by a consistently strong association between abundance of *Heterocapsa* and Chlorophyll-a in the PCA analysis.

4. Discussion

In the Patagonian fjords region of southern Chile (41-51ºS) the phytoplankton community is typically dominated by large diatoms in spring and by nanoflagellates in winter (Iriarte et al., 2007b; Iriarte and González 2008; Czypionka et al. 2011; Montero et al., 2011). To date, the seasonal cycle of phytoplankton productivity has been described in terms of two alternating periods: i) a productive season (typically extending from late August to May) characterized by the periodic occurrence of high rates of GPP (1-3 g C m^{-2} d^{-1}) and ii) a short non-productive season in deep winter (June and July) with much lower rates of GPP (<0.5 g C m^{-2} d^{-1}) (Pizarro et al., 2005; Iriarte et al., 2007b; Montero et al., 2011 and our own unpublished data). This decrease in photosynthetic activity during winter has been associated with the seasonal reduction in light intensity and day length that should inhibit blooming of highly productive diatom populations. Moreover, wind-mixing events in winter tend to distribute diatoms throughout a deeper mixed layer such that the average irradiance limits their photosynthesis and growth.

Here we report for the first time high levels of GPP (0.6-1.6 g C m^{-2} d^{-1}) associated with a dense bloom of the dinoflagellate *Heterocapsa triquetra* during the deep Patagonian winter. This finding contradicts the generally accepted paradigm that low light severely limits GPP rates during the winter in these Patagonian fjords (Iriarte et al., 2007b) and is not consistent with the classical “mandala” that describes a succession of phytoplankton groups culminating in blooms of dinoflagellates (Margalef, 1978).

Blooms of *Heterocapsa* species have also been reported during winter in the northern hemisphere, despite relatively short day lengths and atmospheric systems that bring cloudy conditions and hence significantly reduced incident irradiance (Litaker et al., 2002b). Our PCA analysis showed a weak relationship between *Heterocapsa* and irradiance, perhaps as a result of the ability of this species to tolerate and thrive at the low irradiance levels that characterize winter periods in Chilean fjords (Iriarte & González, 2008; Huovinen et al., 2016). Underwater irradiance was typically in the range of 1-50 µE m^{-2} s^{-1} in the upper 5-10 m, in contrast to much higher irradiance levels (10-500 µE m^{-2} s^{-1}) observed in spring-summer at the same location (Fig. 6). Once established, the abundance peak of the *Heterocapsa triquetra* bloom typically occurred at an irradiance of only 1-10 µE m^{-2} s^{-1} (Fig. 6), which is of the same order of magnitude as typical compensation irradiance levels for dinoflagellates (Richardson et al. 1983). Clearly these low irradiances partly result from self-shading, but the fact that high rates of GPP are maintained by *Heterocapsa triquetra* under such conditions is evidence for a remarkable photosynthetic efficiency at low light that must give this species a competitive edge under these winter conditions. pH values exceeding 8.5, and at times exceeding 9, were observed in association with the high levels of chlorophyll and dissolved oxygen associated with the bloom (Fig. 2) and provide further strong evidence for the high rates of primary productivity observed. This is supported by observations of pH in excess of 9 and a large drawdown in total dissolved inorganic carbon in monocultures of *Heterocapsa triquetra* (Hansen et al. 2007).

Under low light conditions, it has been suggested that mixotrophy by photosynthetic algae could confer an advantage over other phytoplankton species mainly due to the supplementary carbon source to balance low rates of photosynthesis (Legrand et al., 1998; Litaker et al., 2002a; Millette et al., 2017). Mixotrophy in several

species of *Heterocapsa* could be a successful strategy for phagotrophic uptake of nitrogen and phosphorus when these elements are limiting or when light limits photosynthesis (Legrand et al., 1998; Li et al., 1999, Millette et al. 2017). Despite the low irradiance levels recorded, our data suggest that GPP and pH were highest during July 12, co-incident with the peak in abundance of *H. triquetra* and in Chl-*a* concentrations (Fig. 4). However, a decrease in Chl-*a* during July 16, despite the high abundances observed (Fig. 4), suggests that self shading may have been limiting further growth, and therefore a mixotrophic mode of nutrition for the *Heterocapsa* bloom may have been conceivable at this stage of the bloom. Previous studies have indicated that the reduction in cellular Chl-a content in mixotrophic phytoplankton might be the consequence of an increase in growth rate due to feeding (Skovgaard 1996a; Hansen et al., 2000; Skovgaard et al., 2000). We did not measure cellular Chl-a content of individual cells, but we did observe between July 14 and July 16 a decrease in total Chl-a from 149 to 70 mg m^{-2} associated with high *Heterocapsa* abundances of 43 and 40 × 10^9 cell m^{-2}, respectively (Fig. 4). It is therefore possible that *H. triquetra* may have supplemented phototrophy with mixotrophy during the study period. It is interesting that mixotrophy now features as an important functional trait in a recently revised version of Margalef's Mandala (Glibert 2016).

Winter synoptic low-pressure systems (LPS) are associated with heavy rainfall and runoff that can supply inorganic nutrients critical for initiation and development of *Heterocapsa* blooms in the northern hemisphere (Litaker et al., 2002a). In the present study we also linked the bloom of *H. triquetra* to the passage of a synoptic low-pressure system that affected Puyuhuapi Fjord during our sampling campaign. Patagonian fjord ecosystems are generally surrounded by pristine woodland and low human population density, and therefore the increase in river runoff during LPS events does not generally

deliver enhanced concentrations of inorganic nutrients to surface coastal waters, with the exception of silicic acid. The unique characteristics of Patagonian coastal waters mean that nitrate and phosphate concentrations are increased within surface waters (also marked by increases in surface T and S from deeper water) by mixing of the water column as a result of the passage of these LPS events.

The study area was subjected to the passage of several LPS events separated by intervals of two to four days. During these events, stronger northern winds (10-20 m s^{-1}) were recorded, and this contributed to mixing of the water column and the vertical displacement of the pycnocline. We suggest that these mixing and turbulence mechanisms supplied nutrients (nitrate and phosphate) from depth to surface waters, offering favourable conditions for growth of *H. triquetra* (summarized in Fig. 7). High-resolution vertical hydrographic profiles showed evidence for strong mixing in the upper 8 m of the water column that broke down stratification of surface waters (Fig. 3). The impact of LPS events was apparent down to a depth of ~30 m, where nitrate and phosphate were present at higher concentrations (>8 µmol L^{-1} nitrate, >0.6 µmol L^{-1} phosphate) and could be transported into surface waters through vertical mixing (Inall and Gillibrand, 2010; Silva and Vargas, 2014).

During the sampling period a thermal inversion layer covered the upper ~30 m of the water column, a feature of winter conditions caused by heat loss (Schneider et al., 2014), with salinity also increasing with depth owing to fresh water input into surface waters both from the Cisnes River discharge (Fig. 2C), and from rainfall. The presence of this cool-fresh water layer over warmer-salty waters contributed to the occurrence of double diffusive layering (DL) events, which was supported by the presence of multiple thermohaline staircases (Fig. 3F). In Patagonian fjords, this DL is an important process (Pérez-Santos et al., 2013 and 2014) that plays a significant role in vertical mixing of

the water column and consequent injection of nutrients into surface waters. In addition, the dissipation rate of turbulent kinetic energy ($\varepsilon=10^{-5} – 10^{-4}$ W kg^{-1}) and the diapycnal eddy diffusivity were high during the sampling period ($k\rho=10^{-5} – 10^{-4}$ m^2 s^{-1}), highlighting the importance of turbulent mixing in supplying nutrients to surface waters.

Before the occurrence of bloom, the water column was characterized by relatively warmer and saltier surface water, with dissolved oxygen, chl-a and pH values typical of non-productive conditions. However, the passage of LPS (~990 mbar) on July 8 increased wind intensity and vertical mixing. This was followed by an increase in the Cisnes River discharge from 150 m^3 s^{-1} to 608 m^3 s^{-1} and a decrease in the surface water temperature and salinity, which stabilized the water column and created conditions favorable for both aggregation and growth of *H. triquetra* (Fig. 7). The low concentrations of nitrate and phosphate in surface water were augmented by vertical exchange with deeper water during the LPS event, and this injection of nutrients presumably satisfied the nutrient demand of the dinoflagellates (Fig. 7). PCA analysis showed an inverse association between abundance of *Heterocapsa* and concentrations of nitrate and phosphate, reflecting the depletion of these nutrients from surface water column by this dominant species.

The high-resolution vertical profiling of fluorescence confirmed a vertical migration pattern in which the population of *H. triquetra* ascended during the early hours of daylight, and then descended during the afternoon; we did not sample during dark hours. This migration behaviour within the pycnocline persisted even during the influence of the strong LPS (although the abundance peak may have been deeper and more dispersed), and may have been related to nutrient uptake, selection of optimal light environment, or both. Clearly, without this vertical migration pattern, much of the

population would have probably been subject to irradiance levels lower than the compensation irradiance and a bloom may not have developed.

Several authors have suggested that small flagellates, and particularly dinoflagellates, dominate phytoplanktonic communities when the water column is stratified (Eppley et al. 1978; Cohen, 1985). In our study, stratification resulted from a large influx of freshwater from the Cisnes River into the fjord, where surface salinities (1-5 m) were between 17 and 25 and temperatures between 8 and 10ºC. *Heterocapsa triquetra* has a wide tolerance to salinity (Mallin, 1994) and the ability to slowly adapt to low temperatures (Baek et al., 2011; Jephson et al., 2011). This physiological plasticity could therefore be directly involved with its capability to form blooms under harsh winter conditions.

Annual production in Puyuhuapi Fjord has been estimated at approximately 250 g C m^{-2} $year^{-1}$, with production in winter contributing only about 6% of this annual value (unpublished data). Blooms of *H. triquetra* as observed in a winter period previously described as non-productive, could therefore contribute significantly to annual productivity. GPP rates reported here were approximately three times higher than generally observed in Chilean fjords during winter, and are more comparable to rates reported during the productive season in Puyuhuapi Fjord (0.5-3 g C m^{-2} d^{-1}; unpublished data), in the Chiloé interior Sea (0.3-1 g C m^{-2} d^{-1}; Iriarte et al., 2007) and in Reloncaví Fjord (0.9-2 g C m^{-2} d^{-1}; Montero et al., 2011).

Here we present the first report of a winter dinoflagellate bloom in the Patagonian fjords. These results improve our understanding of primary productivity cycles and composition of phytoplankton communities in Chilean fjords, and challenge the paradigm of winter as a low-productive period. We therefore reject the hypothesis that low irradiance levels limit the development of dense phytoplankton blooms in

winter in these fjords. Physiological plasticity and behavioural patterns may allow *Heterocapsa triquetra* to tolerate and thrive under conditions of low temperature, low salinity and low light characteristic of the deep Patagonian winter.

Conclusion

- A dinoflagellate bloom dominated by *Heterocapsa triquetra* was observed during austral winter and was associated with high rates of gross primary production.
- The vertical mixing produced by the double diffusive layering events and the impact of low-pressure systems on turbulent mixing favored the development of the *Heterocapsa triquetra* bloom through enhanced supply of nutrients.
- Vertical fluorescence profiles, considered as indicative of *Heterocapsa triquetra* abundance, showed a diurnal pattern of vertical migration above the pycnocline with a double layer distribution during the day. Accumulation of the population close to the surface may have facilitated development of the bloom, despite low irradiance.
- The phytoplankton bloom detected in austral winter challenges the paradigms of winter as a low-productive period and of low levels of irradiance as a key factor limiting phytoplankton blooms. This highlights the importance of synoptic events in the ecosystem productivity of Patagonian fjords.

Acknowledgements

This research was funded by FONDECYT 1131063 and COPAS Sur-Austral (CONICYT PFB-31/2017). Iván Pérez-Santos, is also funded by FONDECYT 11140161.

References

1. Baek, S. H, Ki, J. S., Katano, T., You, K., Park, B. S., Shin, H. H., Shin, K., Kim, Y.O., Han, M. 2011. Dense winter bloom of the dinoflagellate *Heterocapsa triquetra* below the thick surface ice of brackish Lake Shihwa, Korea. Phycological Research 59: 273-285.
2. Barton, A. D., Finkel, Z. V., Ward, B. A., Johns, D. G., Follows, M. J. 2013. On the roles of cell size and trophic strategy in North Atlantic diatom and dinoflagellate communities. Limnol. Oceanogr. 58 (1): 254-266.
3. Casas, B., Varela, M., Bode, A. 1999. Seasonal succession of phytoplankton species on the coast of A Coruña (Galicia, northwest Spain). Bol. Inst. Esp. Oceanogr. 15 (1-4): 413-429.
4. Cassis, D., Muñoz, P., Avaria, S. 2002. Variación temporal del fitoplancton entre 1993 y 1998 en una estación fija del seno Aysén, Chile (45º26′S 73º00′W). Revista de Biología Marina y Oceanografía 37 (1): 43-65.
5. Chaigneau, A., Pizarro, O., 2005. Mean surface circulation and mesoscale turbulent flow characteristics in the eastern South Pacific from satellite tracked drifters. J Geophysical Research, Oceans, 110, C05014, doi:10.1029/2004JC002628.
6. Cohen, R. R. H. 1985. Physical processes and the ecology of a winter dinoflagellate bloom of *Katodinium rotundatum.* Mar. Ecol. Prog. Ser. 26: 135-144.
7. Cuypers, Y., Bouruet-Aubertot, P., Marec, C. Fuda, J.L., 2011. Characterization of turbulence and validation of fine-scale parametrization in the Mediterranean

Sea during BOUM experiment, Biogeosciences Discuss., 8, 8961–8998, doi:10.5194/bgd-8-8961-2011.

8. Czypionka, T., Vargas, C.A., Silva, N., Daneri, G., González, H.E, Iriarte, J.L., 2011. Importance of mixotrophic nanoplankton in Aysén Fjord Southern Chile) during austral winter. Cont. Shelf Res. 31 (3-4), 216-224.
9. Eppley R. W., Koeller, P,, Wallace, G. T. 1978. Stirring influences the photoplankton species composition within enclosed columns of coastal seawater. J. Exp. Mar. Biol. Ecol. 32: 239
10. Glibert, P.M. 2016. Margalef revisited: A new phytoplankton mandala incorporating twelve dimensions, including nutritional physiology. Harmful Algae 55, 25–30. doi:10.1016/j.hal.2016.01.008
11. Goebel, N.L., Wing, S.R., Boyd, P.W., 2005. A mechanism for onset of diatom blooms in a fjord with persistent salinity stratification. Est. Coast. Shelf Sci. 64, 546–560.
12. González, H.E., Calderon, M.J., Castro, L., Clement, A., Cuevas, L.A., Daneri, G., Iriarte, J.L., Lizárraga, L., Martínez, R., Menschel, E., Silva, N., Carrasco, C., Valenzuela, C., Vargas, C.A., Molinet, C., 2010. Primary Production and plankton dynamics in the Reloncaví Fjord and the Interior Sea of Chiloé, Northern Patagonia, Chile. Mar. Ecol. Prog. Ser. 402, 13-30.
13. Hansen, P.J., Lundholm, N., Rost, B. 2007. Growth limitation in marine red-tide dinoflagellates: effects of pH versus inorganic carbon availability. Marine Ecology Progress Series 334, 63–71.
14. Hansen, P.J., Skovgaard, A., Glud, R.N., Stoecker, D. N. 2000. Physiology of the mixotrophic dinoflagellate *Fragilidium subglobosum*. II. Effects of time

scale and prey concentration on photosynthetic performance. Mar Ecol Prog Ser 201: 137–146.

15. Huovinen, P., Ramírez J., Gómez I., 2016. Underwater Optics in Sub-Antarctic and Antarctic Coastal Ecosystems. PLoS ONE 11(5): e0154887. doi:10.1371/journal.pone.0154887.
16. Inall, M. E. and Gillibrand, P. A., 2010. The physics of mid-latitude fjords: a review, Geological Society, London, UK, Special Publications 344, 17–33.
17. Iriarte, J. L., Quiñones, R. A., González, R. R. 2005. Relationship between biomass and enzymatic activity of a bloom-forming dinofalgellate (Dinophyceae) in southern Chile (41ºS): a field approach. J. Plankton Res. 27 (2): 159-166.
18. Iriarte, J. L., Quiñones, R. A., González, R.R., Valenzuela, C. P. 2007 a. Relación entre actividad enzimática y biomasa de ensambles fitoplanctónicos en el sistema pelágico. Invest. Mar. 35 (1): 71-84.
19. Iriarte, J. L., González, H. E., Liu, K. K., Rivas, C., Valenzuela, C. P. 2007 b. Spatial and temporal variability of chlorophyll and primary productivity in surface waters of southern Chile. Estuarine, Coastal and Shelf Science 74: 471-480.
20. Iriarte, J.L., Gonzalez, H.E., 2008. Phytoplankton bloom ecology of the inner Sea of Chiloé, Southern Chile. Nova Hedwigia, Beiheft 133, 67–79.
21. Iriarte, J.L., Pantoja, S., González, H.E., Silva, G., Paves, H., Labbé, P., Rebolledo, L., Van Ardelan, M., Häussermann, V., 2013. Assessing the micro-phytoplankton response to nitrate in Comau Fjord (42ºS) in Patagonia (Chile), using a microcosms approach. Environ. Monit. Assess. 185, 5055-5070. doi 10.1007/s10661-012-2925-1

22. Jephson, T., Fagerberg, T., Carlsson, P., 2011. Dependency of dinoflagellate vertical migration on salinity stratification. Aquatic Microbial Ecology 63: 255-264.

23. Lee, C. K., Lee, O. H. and Lee, S. G. 2005. Impacts of temperature, salinity and irradiance on the growth of ten harmful algal bloom-forming microalgae isolated in Korean coastal water. *The Sea (Journal Korean Society Oceanography)* (In Korean) 10: 79–91.

24. Legendre, L., Rassoulzadegan, F. 1996. Food-web mediated export of biogenic carbon in oceans: hydrodynamic control. Mar. ecol. Prog. Ser. 145: 179-193.

25. Legendre, L. 1990. The significance of microalgal blooms for fisheries and for the export of particulate organic carbon in oceans. J. Plankton. Res. 12(4) 681-699.

26. Legrand, C., Granéli, E., Carlsson, P. 1998. Induced phagotrophy in the photosynthetic dinoflagellate *Heterocapsa triquetra*. Aquatic Microbial Ecology 15, 65–75.

27. Li, A., Stoecker, D. N., Adolf, J. E. 1999. Feeding, pigmentation, photosynthesis and growth of the mixotrophic dinoflagellate Gyrodinium galatheanum. Aquat Microb Ecol 19: 163–176

28. Litaker, R. W., Tester, P. A., Duke, C. S., Kenney, B. E., Pinckney, J. L., Ramus, J. 2002 a. Seasonal niche strategy of the bloom-forming dinoflagellate *Heterocapsa triquetra.* Mar. Ecol. Prog. Ser. 232: 45-62.

29. Litaker, R. W., Warner, V. E., Rhyne, C., Duke, C. S., Kenney, B. E., Ramus, J., Tester, P. A. 2002 b. Effect of diel and interday variations in light on the cell division pattern and in situ growth rates of the bloom-forming dinoflagellate *Heterocapsa triquetra.* Mar. Ecol. Prog. Ser. 232: 63-74.

30. Luketina, D. A., Imberger, J., 2001. Determining Turbulent Kinetic Energy Dissipation from Batchelor Curve Fitting. J. Atmos. Oceanic Technol., 18, 100–113, doi: 10.1175/1520-0426.

31. Mallin, M. A., Paerl, H. W., Rudek, J. 1991. Seasonal phytoplankton composition, productivity and biomass in the Neuse River estuary, North Carolina. Estuarine, Coastal and Shelf Science. 32: 609-623.

32. Mallin, M. A. 1994. Phytoplankton ecology of North Carolina Estuaries. Estuaries 17 (3): 561-574.

33. Margalef, R. Life-forms of phytoplankton as survival alternatives in an unstable environment. 1978. Oceanol. Acta 1(4): 493-509.

34. Marshall, H. G., Burchardi, L., Lacouture, R. 2005. A review of phytoplankton composition within Chesapeake bay and its tidal estuaries. J. Plankton. Res 27 (11): 1083-1102.

35. Millette, N. C., Stoecker, D. K., Pierson, J. J. 2015. Top-down control by micro- and mesozooplankton on winter dinoflagellate blooms of *Heterocapsa rotundata*. Aquat. Microb. Ecol. 76: 15-25.

36. Millette, N.C., Pierson, J.J., Aceves, A., Stoecker, D.K. 2017. Mixotrophy in *Heterocapsa rotundata*: A mechanism for dominating the winter phytoplankton. Limnology and Oceanography 62, 836–845. doi: 10.1002/lno.10470

37. Montero, P., Daneri, G., González, H.E., Iriarte, J.L., F.J., Tapia, F.J. Lizárraga, L., Sanchez, N., Pizarro, O., 2011. Seasonal variability of primary production in a fjord ecosystem of the Chilean Patagonia: implications for the transfer of carbon within pelagic food webs. Continental Shelf Research 31, 202 – 215.doi:10.1016/j.csr.2010.09.003

38. Osborn, T. R., 1980. Estimates of the local rate of vertical diffusion from dissipation measurements, J. Phys. Oceanogr., 10, 83–89.

39. Parsons, T.R., Maita, Y., Lalli, C.M., 1984. Counting, media and preservatives. Chapter 8. In: A manual of chemical and biological methods for seawater analysis (pp. 173). Pergamon Press, Toronto.

40. Pérez-Santos, I., Vargas, J.G., Schneider, W., Parra, S., Ross, L. & Valle-Levinson, A. 2013. Double diffusion from microstructure measurements in the Martínez and Baker channels, central Chilean Patagonia (47.85°S), Lat. Am. J. Aquat. Res., 41(1), DOI: 103856/vol41-issue1-fulltext-x.

41. Pérez-Santos, I., Garcés-Vargas, J., Schneider, W., Ross, L., Parra, S. & Valle-Levinson A., 2014. Double-diffusive layering and mixing in Patagonia fjords, Progress in Oceanography, 129, 35-49.

42. Pizarro, G., Astoreca, R., Montecino, V., Paredes, M.A., Alarcón, G., Uribe, P., Guzmán, L., 2005. Patrones espaciales de la abundancia de la clorofila, su relación con la productividad primaria y la estructura de tamaños del fitoplancton en Julio y Noviembre de 2001 en la región de Aysén (43°-46°S). Rev. Cien. Tecn. Mar. 28(2), 27-42.

43. Richardson, K., Beardall, J., Raven, J.A. 1983. Adaptation of unicellular algae to irradiance: an analysis of strategies. New Phytol. 93, 157–191.

44. Ruddick, B.R., 1983. A practical indicator of the stability of the water column to double-diffusive activity. Deep-Sea Research 30, 1105–1107.

45. Ruddick, B., Anis, A., Thompson, K., 2000. Maximum Likelihood Spectral Fitting: The Batchelor Spectrum. J. Atmos. Oceanic Technol., 17, 1541–1555, doi: 10.1175/1520-0426.

46. Schneider, W., Pérez-Santos, I., Ross, L., Bravo, L., Seguel, R., Hernández, F., 2014. On the hydrography of Puyuhuapi Channel (Chilean Patagonia). Progress in Oceanography 129, 8-18. doi10.1016/j.pocean.2014.03.007

47. Sellner, K. G., Lacouture, R. V., Cibik, S. J., Brindley, A. and Brownlee, S. G., 1991. Imporantance of a winter dinoflagellate-microflagellate bloom in the Patuxent river estuary. Estuarine, coastal and shelf science, 32, 27-42.

48. Shih, L. H., Koseff, J. R., Ivey, G. N., Ferziger, J., 2005. Parameterization of turbulent fluxes and scales using homogeneous sheared stably stratified turbulence simulations, J. Fluid Mech., 525, 193–214.

49. Sievers, H., Silva, N., 2008. Water masses and circulation in austral Chilean channels and fjords. Progress in the Oceanographic Knowledge of Chilean Interior Waters, from Puerto Montt to Cape Horn, Comité Oceanográfico Nacional – Pontificia Universidad Católica de Valparaíso, Valparaíso, pp. 53–58.

50. Silva, N., 2008. Dissolved oxygen, pH, and nutrients in the austral Chilean channels and fjords. Progress in the oceanographic Knowledge of Chilean interior waters, from Puerto Montt to Cape Horn. N. Silva & S. Palma (eds.) Comité Oceanográfico Nacional – Pontificia Universidad Católica de Valparaíso, Valparaíso, pp. 37–43.

51. Silva, N. and Vargas, C., 2014. Hypoxia in Chilean Patagonia fjords, Progress in Oceanography, Vol. 129, 62-74.

52. Skovgaard, A. 1996a. Mixotrophy in *Fragilidium subglobosum* (Dinophyceae): growth and grazing responses as functions of light intensity. Mar Ecol Prog Ser 143: 247–253.

53. Skovgaard, A., Hansen, P. J., Stoecker, D. K. 2000. *Fragilidium subglobosum*. I. Effects of phagotrophy and irradiance on photosynthesis and carbon content. Mar Ecol Prog Ser 201: 129–136

54. Strickland, J.D.H., Parsons, T.R., 1968. A Practical Handbook of Seawater Analysis. Bull. Fish. Res. Board Can. 167.

55. Strickland, J.D.H., 1960. Measuring the production of marine phytoplankton. Bull. Fish. Res. Board Can. 122, 1 – 172.

56. Tas, S. 2015. A prolonged red tide of *Heterocapsa triquetra* (Ehrenberg) F. Stein (Dinophyceae) and phytoplankton succession in a eutrophic estuary (Turkey). Medit. Mar. Sci. 16 (3): 621-627.

57. Torres, R., Silva, N., Reid, B., Frangopulos, M., 2014. Silicic acid enrichment of subantarctic surface water from continental inputs along the Patagonian archipelago interior sea (41–56ºS). Progress in Oceanography 129, 50–61. doi:10.1016/j.pocean.2014.09.008

58. Thorpe, S. A., 2005. The turbulence ocean. Cambridge Universty Press, CB2 2RU, UK, 426 pp.

59. Utermöhl, H., 1958. Zur Vervollkommnung der quantitativen Phytoplankton-Methodik. Internationale Vereinigung für Theoretische und Angewandte Limnologie. Komitee für Limnologische Methoden. 9: 1–39.

60. Williams, P. J. LeB., Robertson, J.E., 1991. Overall planktonic oxygen and carbon dioxide metabolisms: the problem of reconciling observations and calculations of photosynthetic quotients. Journal of Plankton Research 13 (suppl.),153–169.

61. Yamaguchi, M., Itakura, S., Nagasaki, K., Matsuyama, Y., Uchida, T., Imai, I. 1997. Effects of temperature and salinity on the growth of the ride tide

flagellates *Heterocapsa circularisquama* (Dinophyceae) and *Chatonella verruculosa* (Raphidophyceae). J. Plankton. Res. 19 (8): 1167-1174.

62. You, Y., 2002. A global ocean climatological atlas of the Turner angle: implications for double-diffusion and water-mass structure, Deep-Sea Research I 49, 2075–2093.

Figure captions

Fig. 1. (A) Infrared image of GOES-13 showing the influence of low pressure systems in Patagonian region. (B) Study area in Puyuhuapi Fjord.

Fig. 2. (A-E) Wind speed (A) and air pressure (B) data in July 2015 taken from the meteorological station in Magdalena Island, located 900 m from the buoy position. (C) Cisnes River discharge. D-H represents temperature, salinity, dissolved oxygen, chlorophyll-a (fluorescence) and pH logged hourly in surface water at the Puyuhuapi buoy in July, 2015.

Fig. 3. High vertical resolution of physical properties from SCAM microprofiler showing the temperature (A), salinity (B), density (C), buoyancy frequency (D), temperature gradient (E), Turner angle (F), dissipation rate of turbulent kinetic energy (G) and the diapycnal eddy diffusivity (H) obtained before and after the passage of low pressure system.

Fig. 4. (A) Total abundance of phytoplankton taxonomic groups combined with gross primary production GPP and (B) size- fractionated chlorophyll-a data.

Fig. 5. (A) Principal component analysis (PCA) carried out between the dominant phytoplankton species and the physical and chemical parameters. (B) Correlations between principal components (1 and 2) and log-transformed GPP values.

Fig. 6. Vertical profiles of fluorescence and underwater irradiance (photosynthetically active radiation, PAR) during July 2015. To the right are comparable profiles for austral summer 2014 and 2013 at the same location. In the lower panels, the depths of the occurrence of 1 and 10 $\mu E\ m^{-2}\ s^{-1}$ levels are shown to approximate the compensation irradiance zone for dinoflagellates.

Figure 7. Conceptual diagram showing the putative processes occurring during the development of the bloom.

Supplementary material caption

Fig. 1. Time evolution of high resolution vertical profiles of temperature, salinity, density and fluorescence from SCAMP microprofiler and in-situ phytoplankton sampling during (colour bars) July 12, 2015, (Upper panel) and July 15, 2015 (Lower panel).

Fig. 2. Time evolution of high resolution vertical profiles of temperature, salinity, density and fluorescence from SCAMP microprofiler and in-situ phytoplankton sampling during (colours bars) July 16, 2015.

Table 1. Nutrient concentrations, Total Phytoplankton Abundance, Chlorophyll-a (chl-a), Gross Primary Production (GPP), Temperature (T), Salinity (S) and Irradiance (PAR) measured at different depths (Z) during the study period. The fluorescence data shown on July 10 corresponds to the profile taken on July 11.

			µM	µM	µM	$\cdot 10^3$ cell mL^{-1}	mg L^{-1}	mg m^{-3}	mmol O_2 m^{-3} d^{-1}	ºC	PPT	µE m^{-2} sec^{-1}
Date	Station	Z	NO_3	PO_4	$Si(OH)_4$	Abundance	Chl-a TOTAL	Fluorescence	GPP	T	S	PAR
10-Jul-15	BOYA	1	3.8	0.1	37.9	3.3	11.0	11.8	7.5	8.5	18	26.5
		5	10.0	0.1	32.7	1.2	6.7	2.2	2.6	9.7	25	7.7
		15	15.8	0.6	22.5	0.03	1.7	1.0	3.9	10.5	29	1.1
		50	15.6	1.1	19.3							
		100	11.1	0.9	29.5							
12-Jul-15	BOYA	2	1.1	0.2	49.8	8.6	28.5	73.7	31.4	7.9	17	2.9
		5	4.0	0.1	48.9	5.0	5.1	5.4	8.6	9.1	21	0.9
		15	8.5	0.6	36.5	0.2	1.7	1.1	0.2	10.1	28	0.1
		50	8.9	1.1	26.5							
		100	12.9	1.1	49.6							
14-Jul-15	BOYA	2	1.3	0.1	65.0	4.2	9.5	3.5	15.9	7.9	18	5.9
		5	3.1	0.2	55.8	4.7	14.6	16.8	11.8	8.8	22	1.0
		15	11.2	0.8	33.7	0.4	4.2	1.0	0.3	10.2	29	0.1
		50	13.4	1.8	18.8							
		100	20.4	1.4	27.6							
16-Jul-15	BOYA	2	2.9	0.2	70.6	3.8	3.5	5.3	6.7	8.0	19	6.8
		5	6.1	0.2	43.0	3.4	6.7	8.6	8.6	8.6	23	2.0
		15	14.1	0.9	31.5	0.7	2.9	1.2	9.4	10.2	29	02
		50	13.8	1.1	27.5							
		100	20.7	1.0	59.6							

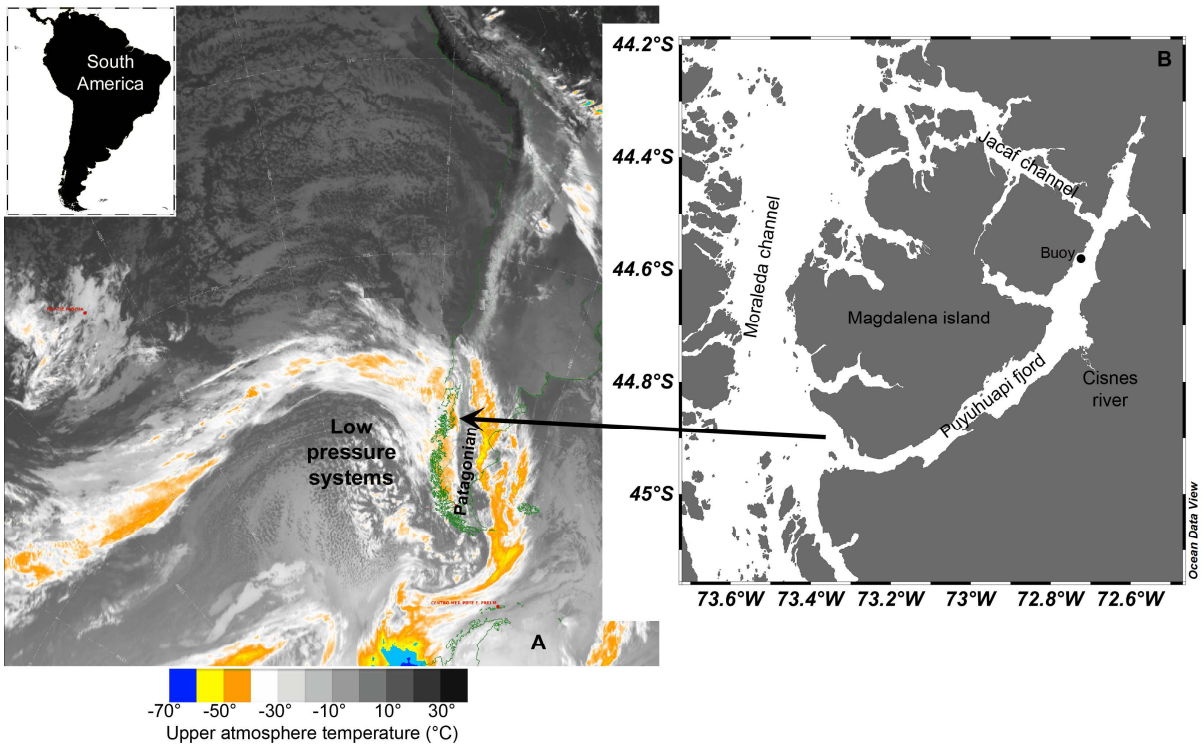

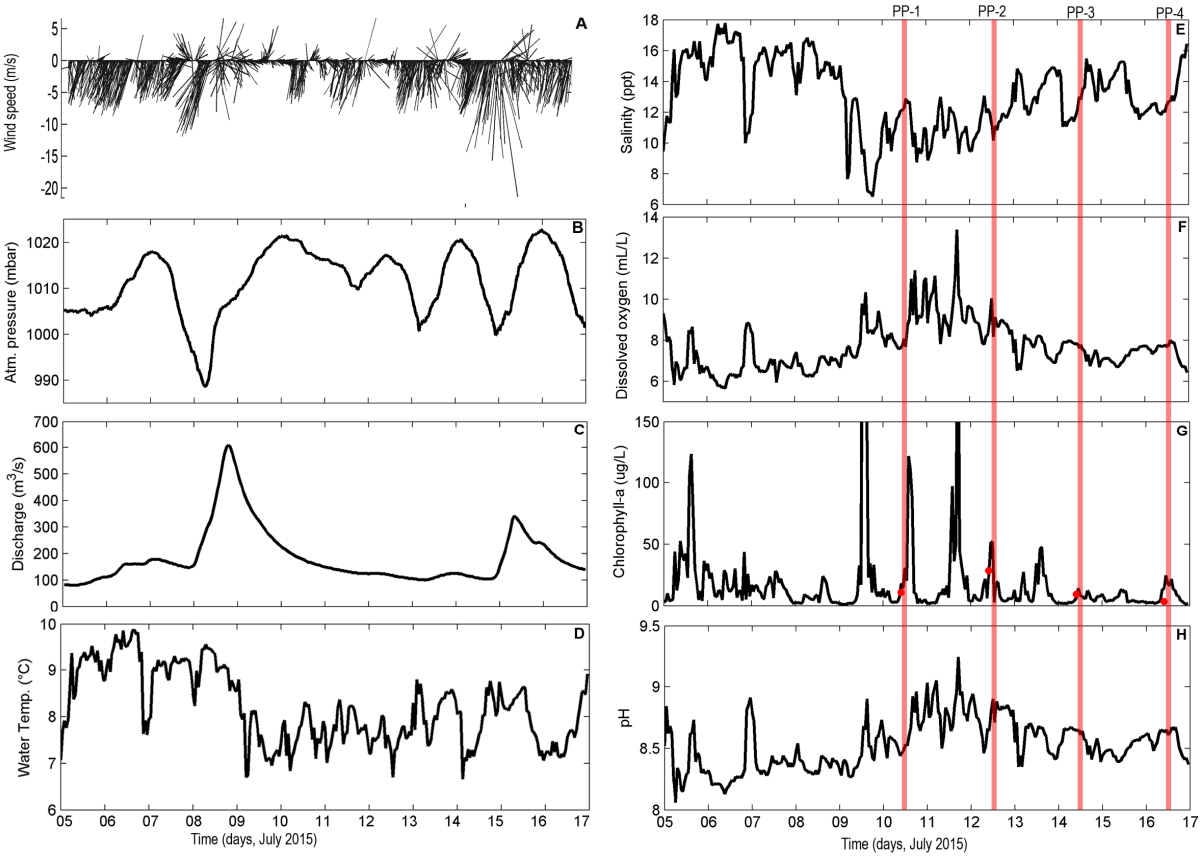

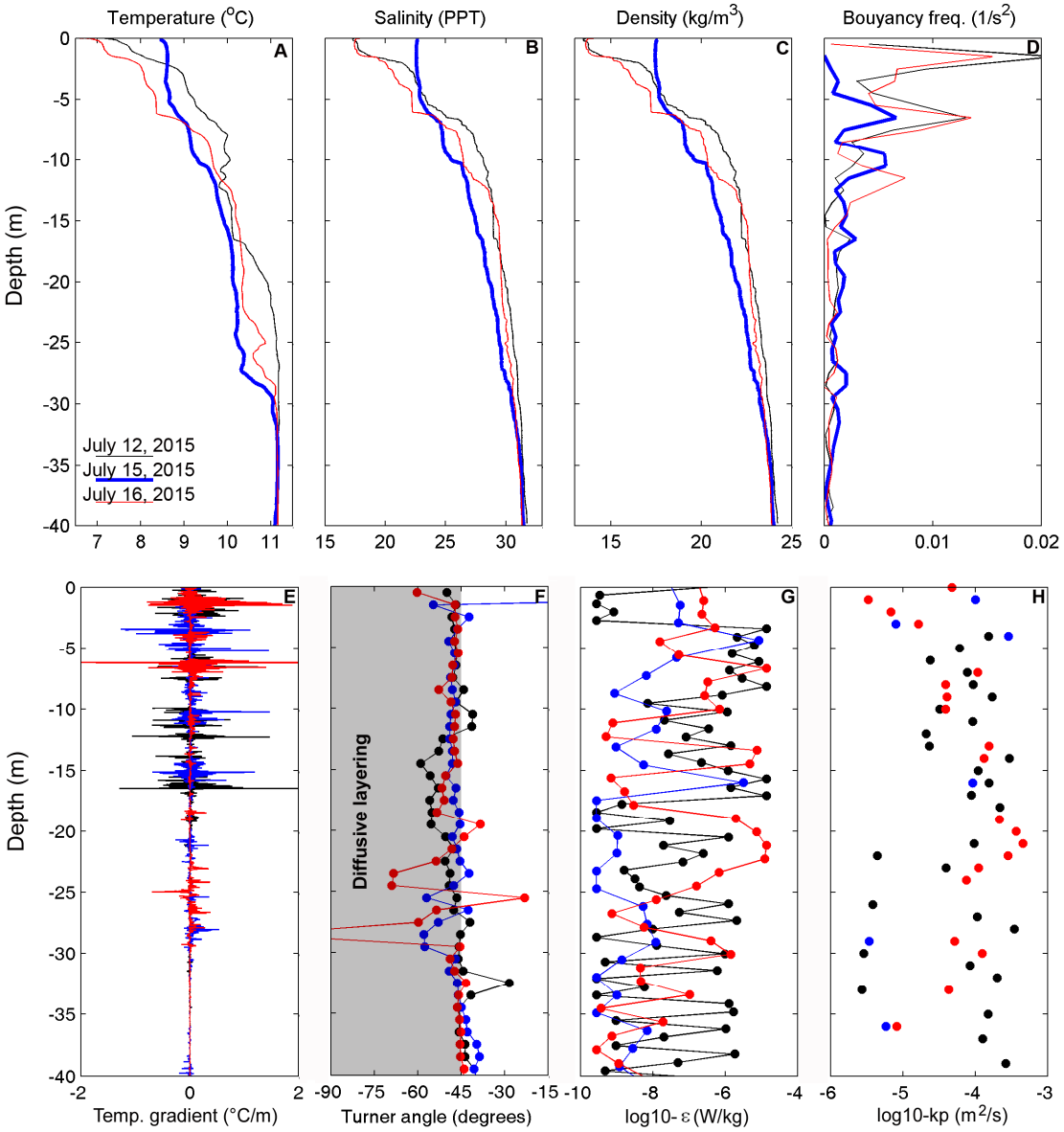

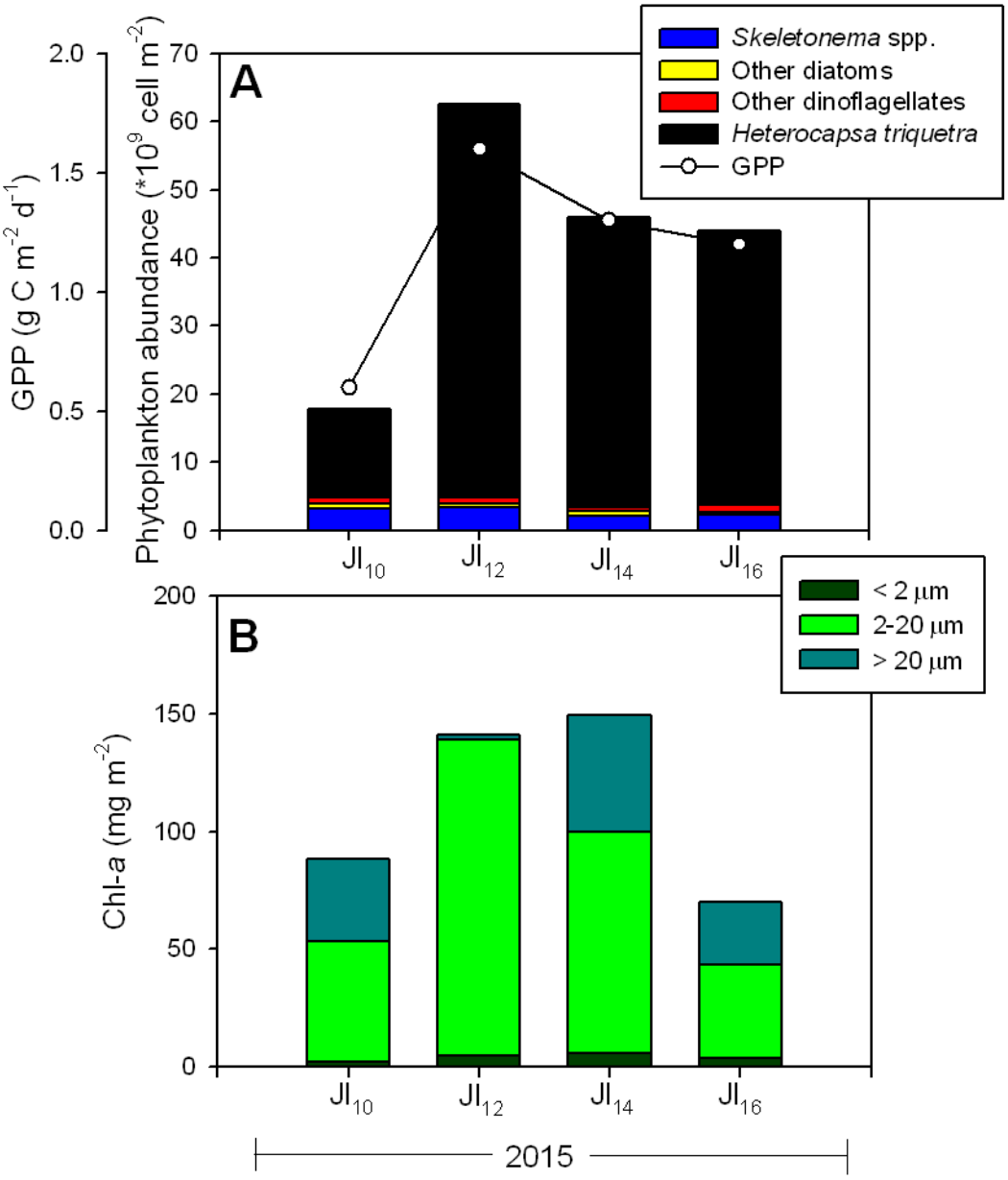
A
Skeletonema spp.
Other diatoms
Other dinoflagellates
Heterocapsa triquetra
GPP
GPP (g C m-2 d-1)
Phytoplankton abundance (*10^9 cell m-2)
2.0
1.5
1.0
0.5
0.0
70
60
50
40
30
20
10
0
JI10
JI12
JI14
JI16
B
< 2 µm
2-20 µm
> 20 µm
Chl-a (mg m-2)
200
150
100
50
0
JI10
JI12
JI14
JI16
2015

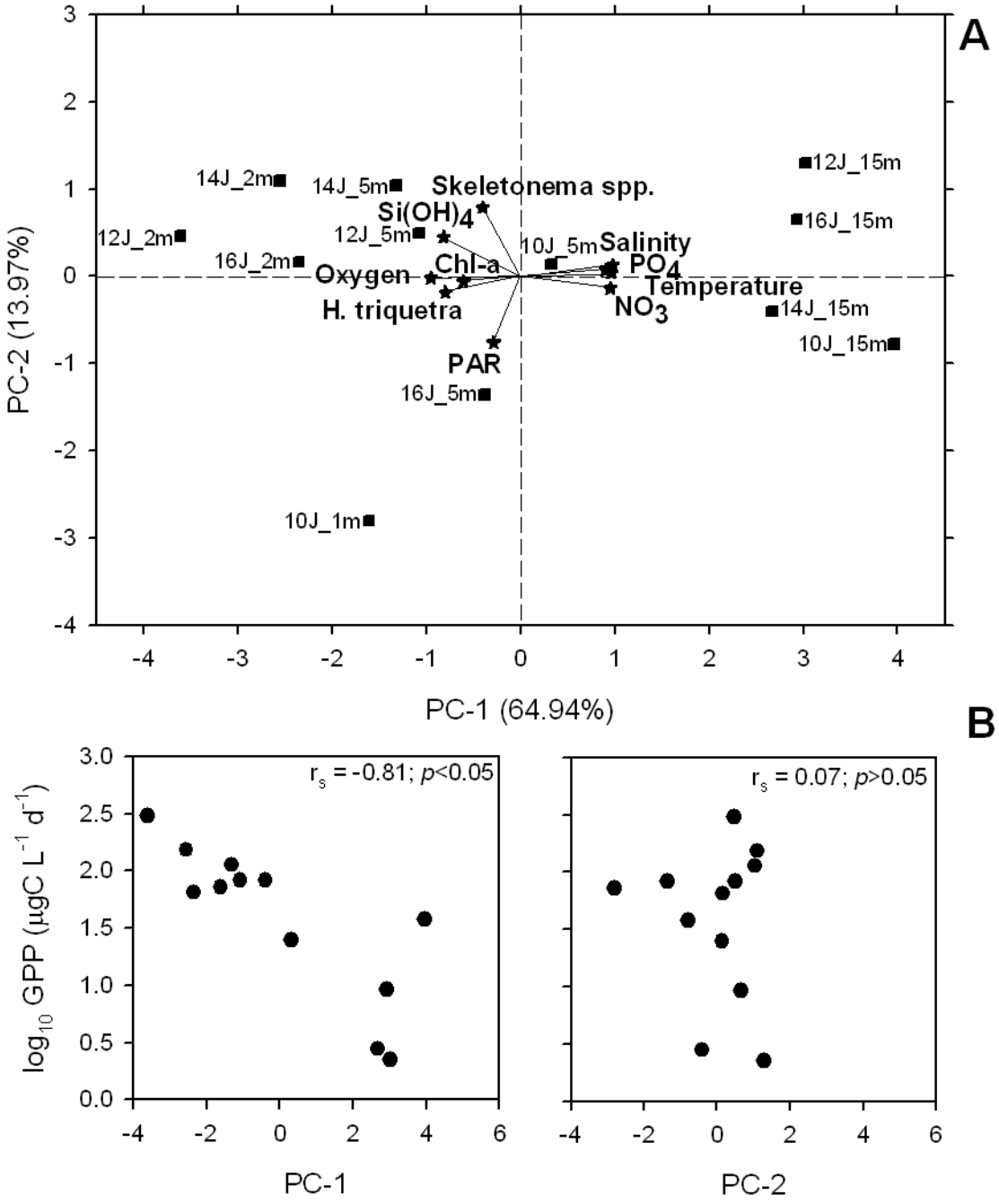
A
PC-2 (13.97%)
PC-1 (64.94%)
14J_2m
14J_5m
Skeletonema spp.
Si(OH)4
12J_15m
16J_15m
12J_2m
12J_5m
10J_5m
Salinity
16J_2m
Oxygen
Chl-a
PO4
Temperature
H. triquetra
NO3
14J_15m
10J_15m
PAR
16J_5m
10J_1m
B
log10 GPP (µgC L-1 d-1)
rs = -0.81; p<0.05
rs = 0.07; p>0.05
PC-1
PC-2

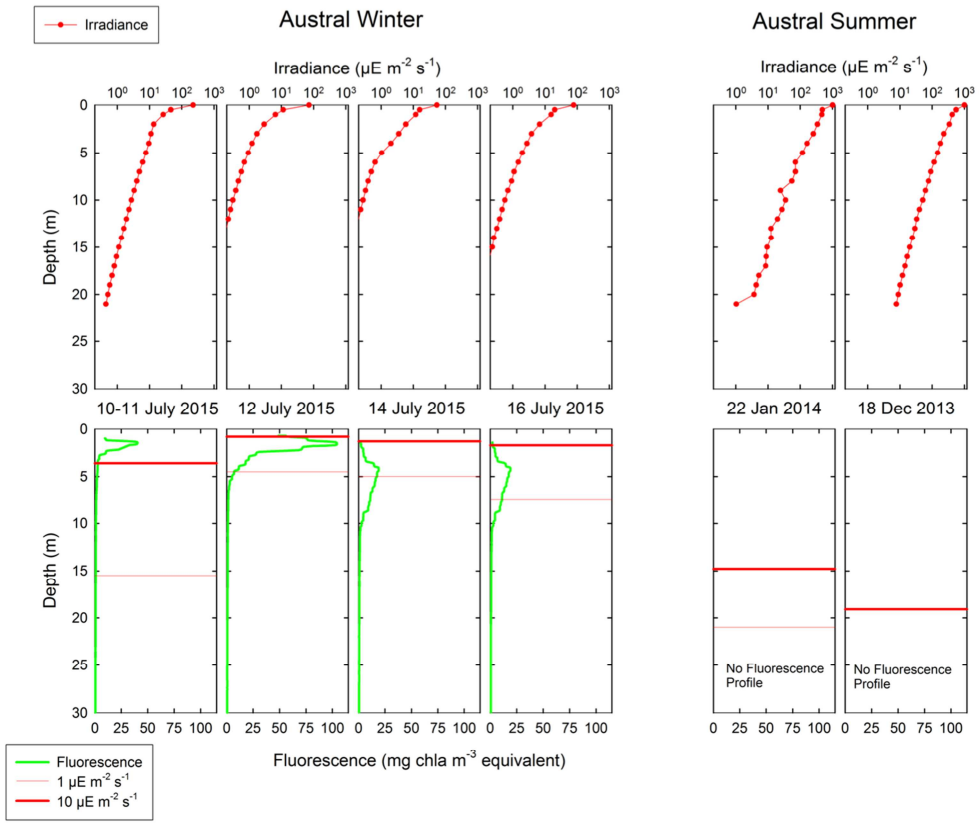

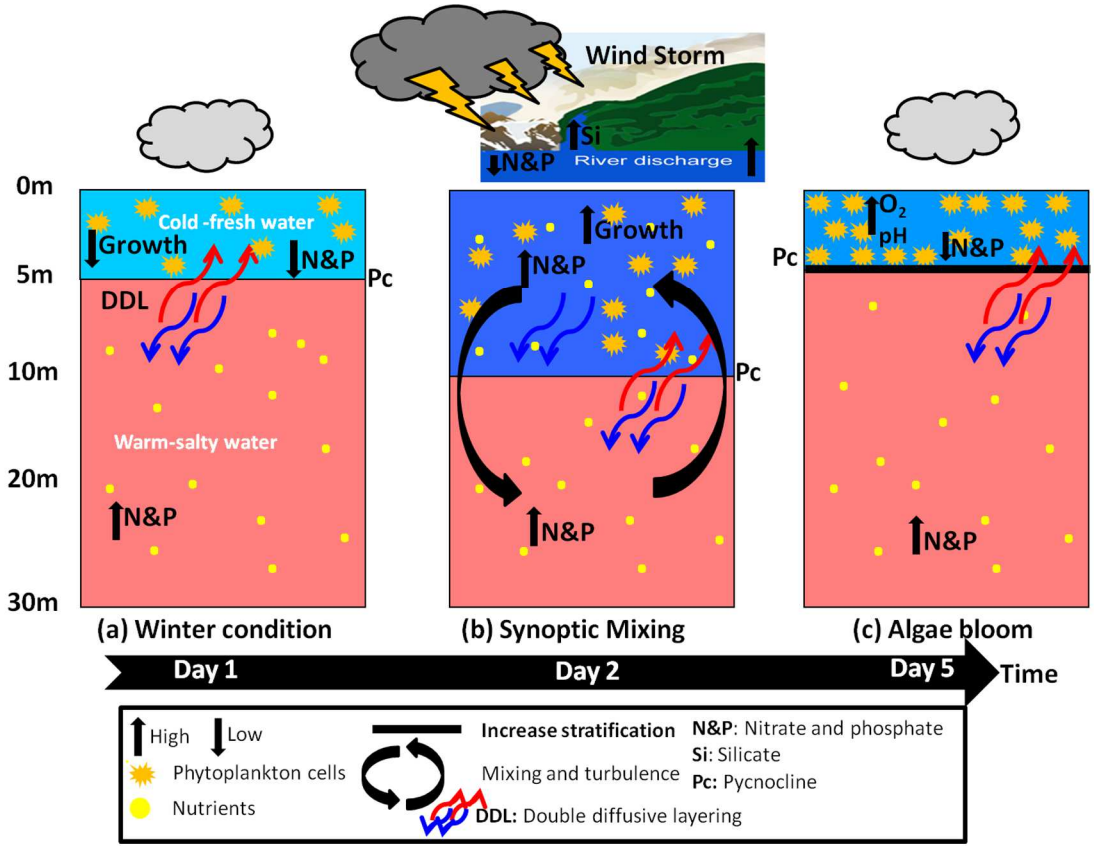

- The dinoflagellate *Heterocapsa triquetra* bloomed in austral winter in a Chilean fjord
- Productivity and biomass were comparable to spring diatom blooms in Patagonian fjords
- The dense bloom developed despite low irradiance levels observed in austral winter